23 Dec 2013

Effect Of Nanoparticles On The Biochemical And Behavioral Aging Phenotype Of The Nematode Caenorhabditis Elegans

Andrea Scharf
Missouri University of Science and Technology, scharfa@mst.edu

Annette Piechulek

Anna Von Mikecz

Recommended Citation

A. Scharf et al., "Effect Of Nanoparticles On The Biochemical And Behavioral Aging Phenotype Of The Nematode Caenorhabditis Elegans," *ACS Nano*, vol. 7, no. 12, pp. 10695 - 10703, American Chemical Society, Dec 2013.
The definitive version is available at https://doi.org/10.1021/nn403443r

Effect of Nanoparticles on the Biochemical and Behavioral Aging Phenotype of the Nematode *Caenorhabditis elegans*

Andrea Scharf, Annette Piechulek, and Anna von Mikecz*

IUF-Leibniz Research Institute for Environmental Medicine, Heinrich-Heine-University Duesseldorf, Auf'm Hennekamp 50, 40225 Düsseldorf, Germany,

ABSTRACT Invertebrate animal models such as the nematode *Caenorhabditis elegans* (*C. elegans*) are increasingly used in nanotechnological applications. Research in this area covers a wide range from remote control of worm behavior by nanoparticles (NPs) to evaluation of organismal nanomaterial safety. Despite of the broad spectrum of investigated NP–bio interactions, little is known about the role of nanomaterials with respect to aging processes in *C. elegans*. We trace NPs in single cells of adult *C. elegans* and correlate particle distribution with the worm's metabolism and organ function. By confocal microscopy analysis of fluorescently labeled NPs in living worms, we identify two entry portals for the uptake of nanomaterials *via* the pharynx to the intestinal system and *via* the *vulva* to the reproductive system. NPs are localized throughout the cytoplasm and the cell nucleus in single intestinal, and vulval B and D cells. Silica NPs induce an untimely accumulation of insoluble ubiquitinated proteins, nuclear amyloid and reduction of pharyngeal pumping that taken together constitute a premature aging phenotype of *C. elegans* on the molecular and behavioral level, respectively. Screening of different nanomaterials for their effects on protein solubility shows that polystyrene or silver NPs do not induce accumulation of ubiquitinated proteins suggesting that alteration of protein homeostasis is a unique property of silica NPs. The nematode *C. elegans* represents an excellent model to investigate the effect of different types of nanomaterials on aging at the molecule, cell, and whole organism level.

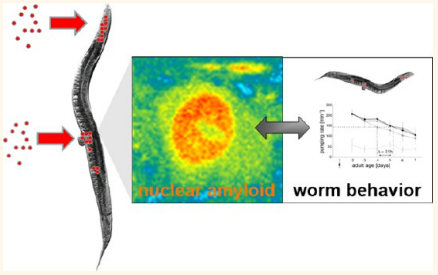

KEYWORDS: aging · amyloid · nanotechnology · nucleolus · pharyngeal pumping · protein aggregation · silica

The nanoparticle–biological interactions are studied using different biological systems such as mammalian cells, daphnia, the fruit fly *Drosophila melanogaster*, the nematode *Caenorhabditis elegans*, fish and rodents.[1−5] *C. elegans* are used for studying nanoparticle (NP) transport and interaction with cells and intestinal organs because they are transparent, allowing optical imaging techniques to visualize the behavior of the NPs *in vivo* for hours to days.[6,7] Metal NPs that accumulate in the worm's organ for food intake, the pharynx, have been used as a remote control to induce retraction behavior through heating.[3] It has also been shown that one can monitor the *in vivo* temperature of *C. elegans* after optical excitation of gold nanoparticles.[8] Furthermore, the biological fitness of an organism can be studied using single and multigenerational approaches that would allow the investigation of the effects of nanomaterials on survival and progeny production.[9,10] Therefore, *C. elegans* present a useful biological model to investigate the nanoparticle–biological interaction.

C. elegans is a free-living, abundant soil nematode that is well-characterized from the molecular to the behavioral level. Sequencing of the *C. elegans* genome was completed in 1998[11] and the complete cell lineage of the worm is defined.[12] Adult worms have about 1000 somatic cells, 302 of which are neurons that are connected by well-known neural circuits and conduct distinct behavioral phenotypes.[13] Since *C. elegans* is transparent throughout its 2 to 3 week long life cycle, labeled macromolecules are detectable in fixed as well as living specimen on the tissue, single cell and subcellular level by differential interference contrast (DIC) and fluorescence microscopy.[14] Thus, imaging of fluorescently labeled NPs allows for correlative investigation of

* Address correspondence to mikecz@tec-source.de.

Received for review July 7, 2013 and accepted November 20, 2013.

Published online November 20, 2013
10.1021/nn403443r

intracellular particle distribution and accumulation with molecular, cellular and behavioral phenotypes in *C. elegans*.

Currently, the use of system biology techniques such as mass spectrometry have provided detailed analysis (e.g., transcriptomes and proteomes) and a better molecular understanding of the nematode genetics, neurobiology, and aging. The investigation of aging mechanisms in *C. elegans* has revealed common pathways that are highly conserved across species. It was shown that inhibition of the insulin/IGF-1/FOXO signaling pathway plays a major role in extension of *C. elegans* lifespan, counteracts aging processes in fruitflies and mammals, and is linked to longevity in human cohorts.[15] Comparative transcriptomes of young *versus* old *C. elegans* have confirmed the importance of insulin-like signaling while additionally showing that down-regulation of heat shock proteins and altered protein homeostasis represent characteristic hallmarks of aging.[16,17] Protein homeostasis that normally is at equilibrium between protein synthesis, folding, localization and degradation seems to decline in the aging nematode. In line with this, mass spectrometry based analyses showed that the proteome of old *C. elegans* contains more insoluble proteins in comparison to young worms and is characterized by aggregation-prone proteins.[18]

We previously showed by differential interference contrast and fluorescence microscopy that silica and polystyrene NPs efficiently translocate to the intestine of *C. elegans via* food intake.[19] Silica NPs induce the egg laying phenotype of an internal hatch, *i.e.*, 'bag of worms', that normally occurs in old *C. elegans* at the end of progeny production and indicates reproductive senescence.[19] A reduction of reproduction was likewise observed after incubation of *C. elegans* with Ag NPs, ZnO NPs, Al_2O_3 NPs, TiO_2 NPs or CdTe QDs NPs,[20−22] yet the underlying mechanisms remain elusive. In this study, we used fluorescence microscopy to trace the movements of NPs in the pharynx, intestine, *spermathecae* and egg laying organ (*vulva*) of living worms. We found that the presence of silica NPs in the respective tissues induces prematurely typical behavioral as well as molecular aging phenotypes of *C. elegans* such as reduced pharyngeal pumping, egg laying and an accumulation of ubiquitinated proteins, *i.e.*, a decline of protein homeostasis. These premature aging phenotypes are NP-specific. Our results suggest that *C. elegans* can be used as a screening platform for nanomaterials, and for the rapid investigation of the nano−bio interactions at the molecular, cellular and behavioral level.

RESULTS/DISCUSSION

Characterization of Particles. Particle size and zeta potential were measured using the Zetasizer Nano-ZS as described in Materials and Methods. The mean sizes of silica, polystyrene or silver NPs were measured by dynamic light scattering. The zeta potential was measured by laser Doppler electrophoresis (Table S1). Intracellular properties and dynamics of silica and polystyrene NPs were characterized using fluorescence correlation microscopy (FCS).[23] FCS analyses clearly showed that intracellular fluorescent signals result from silica and polystyrene NPs and not from detached fluorochromes.[23]

Silica NPs Induce an Insoluble, SDS-Resistant Fraction of Ubiquitinated Proteins. We investigated whether NPs affected age-related changes in the nematode *C. elegans* by analyzing the aging phenotype. The life cycle of *C. elegans* is subdivided into embryonal and larval developmental stages followed by an adult stage of 15−20 days that is characterized by progressive aging. A prominent aging-related molecular phenotype is the increase of insolubility and aggregation of endogenous proteins in aged adult *C. elegans*.[18] To monitor the solubility of proteins, wild-type *C. elegans* were age-synchronized and grown for 24 h in the presence or absence of unlabeled silica NPs (Figure 1A). Filter retardation assays that trap insoluble, SDS-resistant proteins on a cellulose−acetate membrane[24] show that adult *C. elegans* incubated with silica NPs significantly accumulate insoluble, ubiquitinated proteins in comparison to controls which were mock-treated with water only. Quantification of representative dot blots indicates a 2- to 3-fold increase of insoluble, ubiquitinated proteins after 24 h (Figure 1C). These results were compared with protein solubility assays in young (1 day), middle-aged (8 days) and old (12 days) adult *C. elegans* (Figure 1B). Quantification of representative filter retardation assays showed a 3-fold increase of insoluble, ubiquitinated proteins from young to middle-aged animals, and a 4-fold increase of filter-trapped ubiquitinated proteins from young to old worms (Figures 1B, 1C). Thus, exposition of adult *C. elegans* to silica NPs induces a fraction of insoluble, SDS-resistant, ubiquitinated proteins after 24 h that resembles the increase of insoluble, endogenous proteins in old worms.

We next analyzed whether the induction of insoluble protein fractions in *C. elegans* is a NP-specific interaction or else attributable to silica particles in general. Age-synchronized worms were left untreated (H_2O) or treated with unlabeled silica NPs or with BULK-silica (500 nm diameter) for different time periods and subjected to filter retardation analysis (Figure 1D). In contrast to silica NPs, BULK-silica particles do not trap SDS-resistant, ubiquitinated proteins on the filters. The quantification of a representative filter trap experiment shows that signals of BULK-silica-treated worms display similar signal intensities in comparison with untreated controls, whereas silica NPs induce the insoluble ubiquitinated protein fraction 3- to 5-fold after 24 and 48 h (Figure 1E). Thus, the induction of

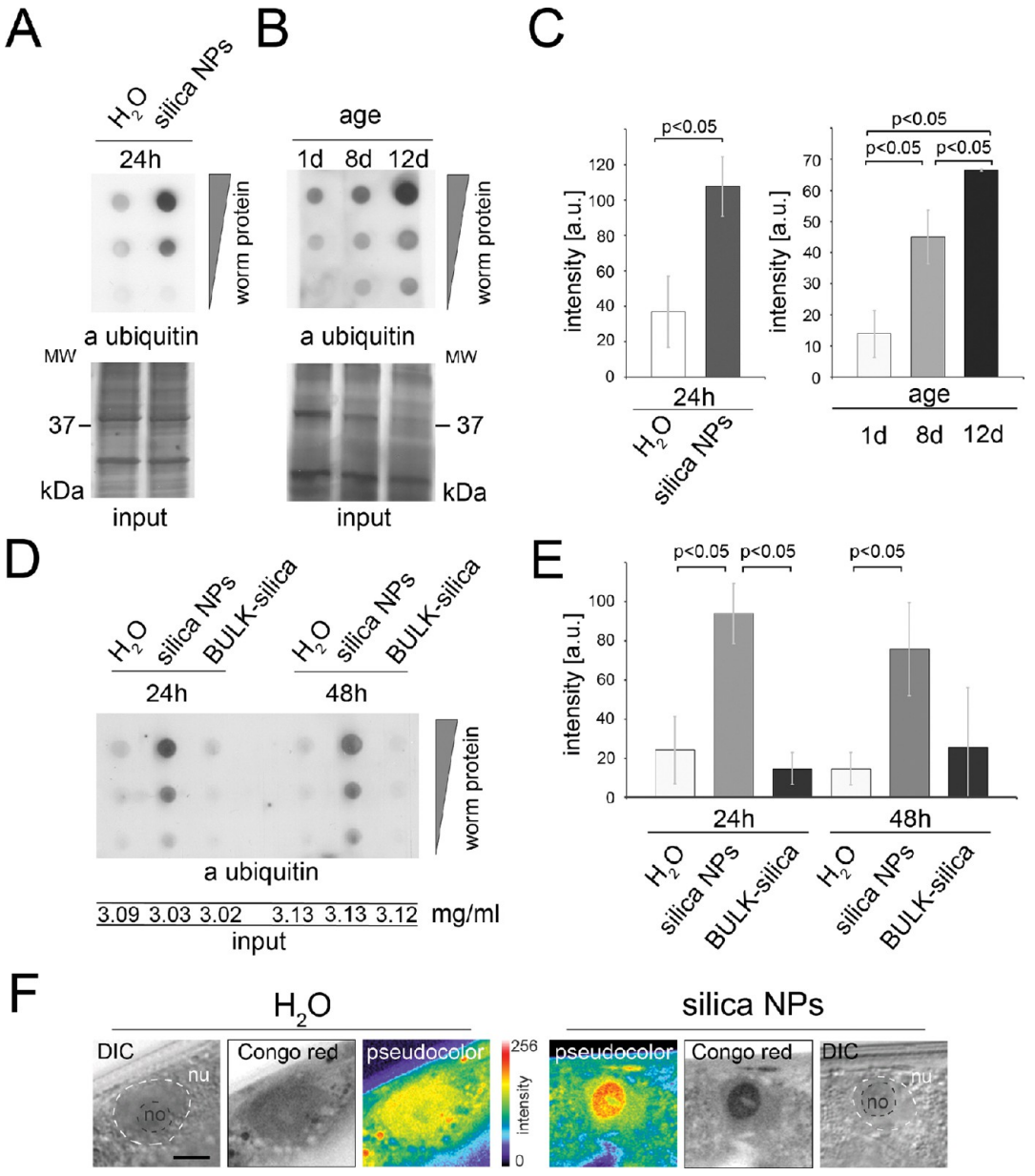

Figure 1. Accumulation of SDS-insoluble, ubiquitinated proteins in *C. elegans*. Filter retardation assays show an accumulation of SDS-insoluble ubiquitinated proteins in *C. elegans* (A) treated with 2.5 mg/mL silica NPs for 24 h in comparison with H_2O as mock-control and (B) with age. As loading controls, total protein extracts were separated by SDS-PAGE, and visualized by silver staining (input). (C) Respective densitometric quantification of filter retardation assays. Values represent means ± SD (H_2O *versus* silica NPs, unpaired Student's *t* test $p < 0.05$; day 1 *versus* day 8 *versus* day 12 worms, one way ANOVA with Tukey post-hoc test $p < 0.05$). (D) Filter retardation assay showing accumulation of SDS-insoluble ubiquitinated proteins in *C. elegans* incubated for 24 and 48 h with H_2O, 2.5 mg/mL silica NPs or 2.5 mg/mL BULK-silica particles (500 nm diameter). (E) Respective densitometric quantification of the filter retardation assays in (D). Values represent means ± SD (24 h H_2O, BULK silica *versus* silica NPs and 48 h H_2O *versus* silica NPs, one way ANOVA with Tukey post-hoc test $p < 0.05$). All filter retardation assays are representative of at least 3 experiments. (F) Fluorescent micrographs of representative anterior-most intestine nuclei of 4-day old, adult *C. elegans* that were mock-treated (H_2O) or treated with 2.5 mg/mL silica-NPs from day 1 of adulthood, fixed and stained with the amyloid-dye Congo red. Congo red staining is shown inverted as gray scale and in pseudocolor as intensity map. a, anti; a.u., arbitrary units; d, days of adulthood; DIC, differential interference contrast; h, hours; kDa, kilodalton; MW, molecular weight; no, nucleolus; nu, nucleus. Bar, 7.5 μm.

protein insolubility constitutes a specific effect of silica NPs on the molecular level.

The identification of aberrant protein aggregation on the global level prompted us to investigate if formation of amyloid-like structures occurs locally. Adult hermaphrodite worms were labeled with the amyloid dye Congo red and observed by confocal microscopy (Figure 1F). Detailed inspection of intestinal cells revealed formation of amyloid-like structures in cell nucleoli of silica NP-treated worms, but not in untreated controls. The results show that silica NPs locally induce fibrillation of endogenous proteins to

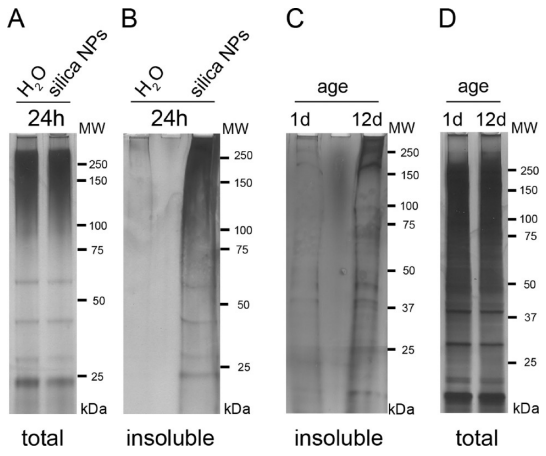

Figure 2. Silica NP-*versus* age-induced SDS-insolubility of *C. elegans* proteins. (A) Total protein extracts or (B) SDS-insoluble proteins eluted from filter retardation assays were from *C. elegans* incubated with 2.5 mg/mL silica NPs or H_2O for 24 h, separated by SDS-PAGE and visualized by silver staining. (C) SDS-insoluble proteins eluted from filter retardation assays and (D) total protein extract of young (1 d) and old (12 d) worms were separated by SDS-PAGE followed by silver staining. The gels are representative for at least 3 independent experiments. d, days; h, hours; kDa, kilodalton; MW, molecular weight.

amyloid-like aggregates in distinct nuclear microenvironments and corroborate the results of the filter trap assays. Notably, this is the first demonstration of endogenous nuclear amyloid formation in *C. elegans*.

Previously it was shown that the global cell fraction of insoluble proteins increases as a hallmark of altered protein homeostasis in aging *C. elegans*.[18] To further investigate protein solubility in silica NP-treated worms, they were left untreated or incubated with unlabeled silica NPs for 24 h, lysed, and subjected to protein separation by gel-electrophoresis (Figure 2). Total cell lysates of untreated and silica NP-treated *C. elegans* display the same band intensities and patterning throughout the complete molecular weight range (Figure 2A). In contrast, the biochemical fractionation of insoluble proteins showed an increase of band intensities of silica NP-treated *versus* untreated worms (Figure 2B). The results indicate that silica NPs selectively induce insoluble proteins, while the soluble protein fraction remains unchanged. This is in line with silica NP-induced accumulation of ubiquitinated proteins in filter retardation assays (Figure 1), and strikingly resembles the growing fraction of insoluble proteins in aging *C. elegans* (Figure 2C,D).[18] Thus, alteration of protein homeostasis toward protein insolubility is identified as a hallmark of *in vivo* interactions between silica NPs and the nematode *C. elegans*. Since protein homeostasis is targeted toward protein insolubility and aggregation similar to aging processes, silica NPs provoke a premature aging phenotype in an organism at the molecular level. Notably, induction of protein aggregation and fibrillation by NPs has been observed before *in vitro*[25] and in cell culture.[26,27] In line

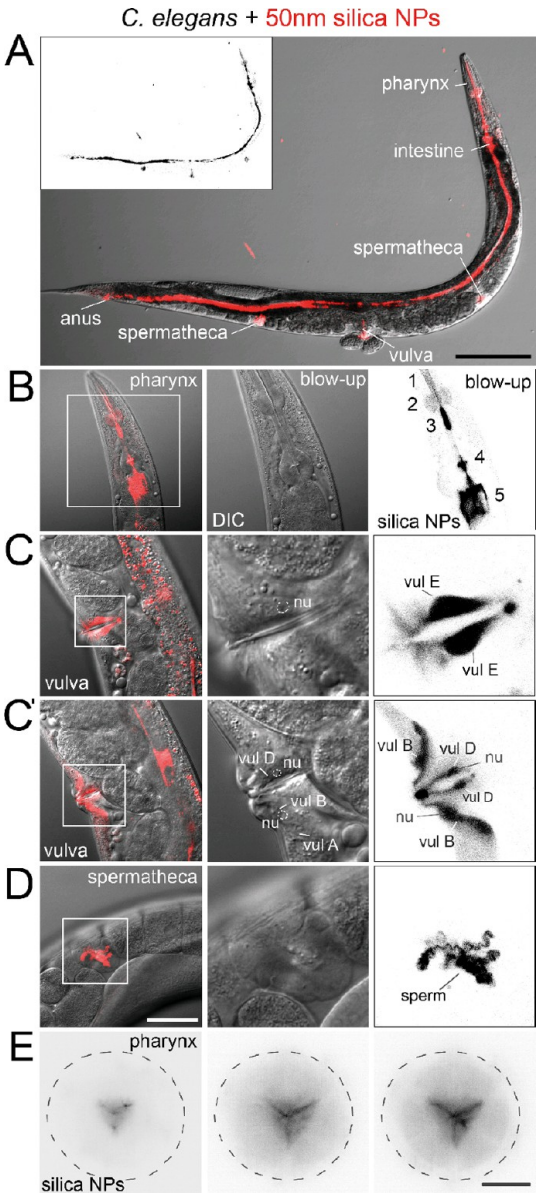

Figure 3. Fluorescently labeled silica-NPs translocate to the pharynx, intestine, *spermatheca*, and *vulva* of living *C. elegans*. (A–E) Fluorescence micrographs of representative 2-day old, adult *C. elegans* that were treated with 2.5 mg/mL rhodamine-labeled silica NPs (red color) for 24 h. (A) Rhodamine-labeled silica NPs are incorporated by the worms through the pharynx or the *vulva* and concentrate in the intestine and *spermathecae*, respectively. The inset shows localization of rhodamine-labeled silica NPs inverted as gray scale. Bar, 100 μm. (B) A representative magnified image of the *C. elegans* head region shows that rhodamine-labeled silica-NPs are localized in all sections of the pharynx: in the (1) procorpus, (2) metacorpus, (3) isthmus, (4) posterior bulb at the grinder, and (5) anterior intestine. (C, C′) Two different lateral sections of the *vulva* show that rhodamine-labeled silica NPs translocate into the cytoplasm and nuclei (nu) of vulval cells vul B, vul D, and vul E. (D) A representative magnificaton of a *spermatheca* shows that rhodamine-labeled silica-NPs are localized at single sperms. Bar, 30 μm. (E) Representative inverted light-sheet microscopic cross sections alongside the dorsal–ventral axis of the pharynx illustrate the translocation of rhodamine-labeled silica-NPs into the tissue of the pharynx. Bar, 10 μm. DIC, differential interference contrast; nu, cell nucleus.

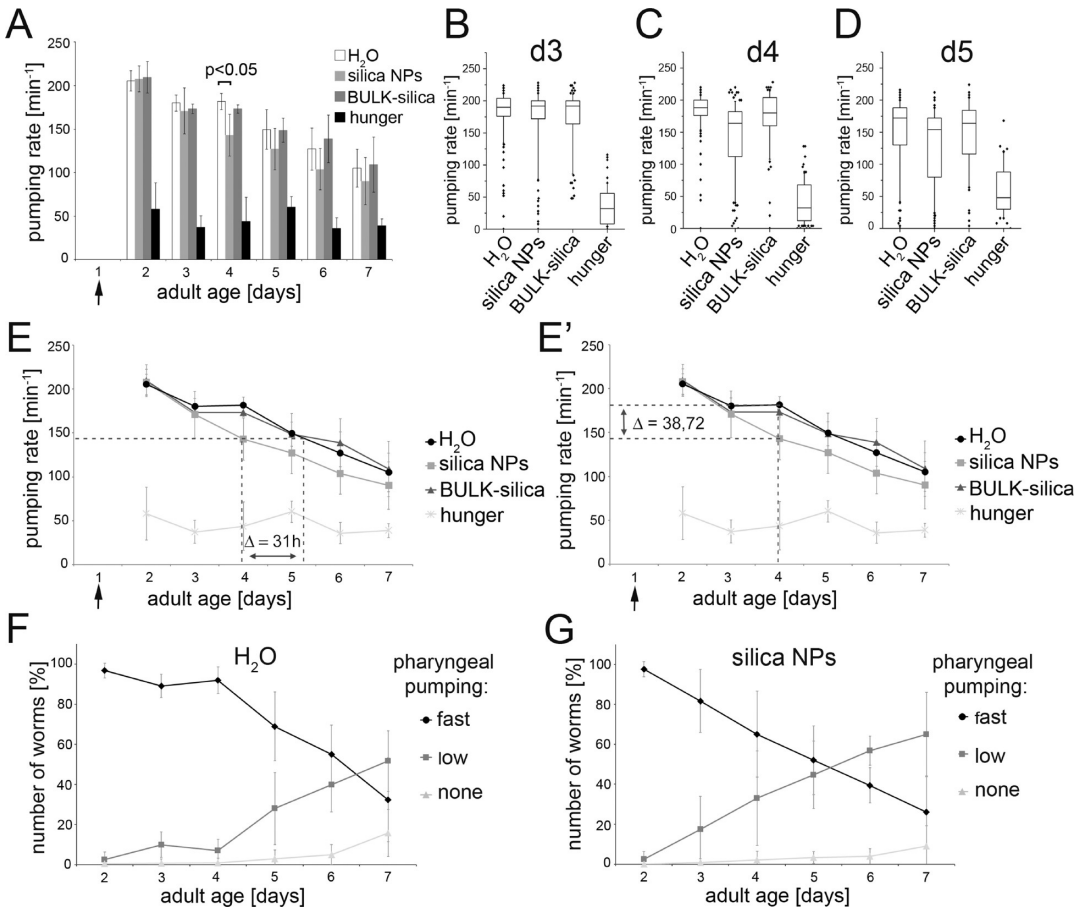

Figure 4. Silica NPs induce a premature decline of pharyngeal pumping. (A) The pharyngeal pumping rate is plotted against age of adult hermaphrodite *C. elegans* (in days) showing a premature decline of pumping in worms treated with silica NPs compared to BULK-silica and H_2O. The arrow indicates the time point of H_2O or particle treatments. In contrast, *C. elegans* that are left without food (hunger) pump with rates around 50 pumps/min that are independent of the worm's age. (H_2O *versus* silica NPs day 4; H_2O, silica NPs and BULK silica *versus* hunger, one way ANOVA with Tukey post-hoc test $p < 0.05$). (B–D) Box blots of the pumping rates shown in (A): (B) 3-day, (C) 4-day, and (D) 5-day old adult hermaphrodites. (E, E′) Graphs illustrate the premature decline of the pumping rate by comparing (E) the age of the worms at which the average pumping rate decreases to 143 pumps/min or (E′) the pharyngeal pumping rate at day 4. (F, G) The plots show age-related changes in the quantity ratio of (F) H_2O- or (G) silica NP-treated worms that are fast-, slow-, or non-pumpers. Values represent means ± SD from at least 3 independent experiments per treatment (H_2O, $n = 160$; silica NPs, $n = 160$; BULK-silica, $n = 115$; hunger, $n = 43$).

with this, it is hypothesized that unique surface properties of NPs sustain protein fibrillation.[28]

Uptake of Silica NPs to the Pharynx, Intestine, Sperms, and Nuclei of Single *Vulva* Cells. Next, the uptake and intracellular accumulation and location of fluorescently labeled silica NPs were investigated in living worms to determine if the effects of the nanomaterial are due to direct interactions between cellular components and the NPs. Differential interference contrast and fluorescence microscopy was chosen for examination of living *C. elegans* to avoid NP wash off due to stringent fixation procedures. Adult hermaphrodite *C. elegans* were fed with rhodamine-labeled silica NPs and observed by confocal microscopy after 24 h (Figure 3). Labeled-NPs distribute throughout the intestine of the worm from the pharynx to the anus, and additionally in the egg laying organ *vulva* and in *spermathecae* (Figure 3A). An increase in the magnification of the image shows that silica NPs concentrate and are traceable in the lumen and organs. In the pharynx, silica NPs translocate to the pharyngeal sections procorpus, metacorpus, isthmus, posterior bulb, and grinder (Figure 3B). In the *vulva* of living *C. elegans*, the distribution of silica NPs is observable intracellularly in single vulval cells, *i.e.*, vul B, vul D, and vul E (Figure 3C,C′). Moreover, confocal sectioning of the lateral view detects labeled silica NPs within the nuclei of vul B and vul D cells (Figure 3C′, nu). Notably, nuclear import of NPs has been observed in cell culture before,[23,26,29] but is now being corroborated for silica and polystyrene NPs *in vivo*, in a living organism (Figure S2). In *spermathecae* of *C. elegans*, silica NPs label single sperms (Figure 3D). Light sheet microscopy confirms that labeled silica NPs translocate to pharyngeal tissue rather than being confined to the pharyngeal lumen (Figure 3F).

The results of the localization study suggest that the silica NPs distribute and accumulate through the entire worm from the tissue to the subcellular level.

Time kinetic experiments show that this particle distribution is stable throughout the worm for at least 48 h (Figure S3). Similar stability of nanomaterials in *C. elegans* was observed after feeding with fluorescently labeled quantum dots.[22,30] Interestingly, rhodamine-labeled silica NPs were not detectable in developing eggs. Rather, the internal hatch of adult worms with the respective egg laying defect feeds on silica NPs within the parent (Figure S4, arrows); *i.e.*, the next generation is likewise mainly exposed *via* food intake. Feeding of adult *C. elegans* with rhodamine-labeled BULK-silica particles shows that particles with a diameter of 500 nm efficiently translocate to and remain within the intestinal lumen of the worms and coat the extracorporal surface of the *vulva* (Figure S5). These results confirm that a mere presence of (nano)-particles in the intestinal lumen of *C. elegans* or on the external surface of the *vulva* are not sufficient to induce the molecular phenotype of amyloid-like protein aggregation. Consistent with this, specific biointeractions of NPs that coat the cuticle, *i.e.*, external surface of the worms[31] are currently unknown.

Silica NPs Induce a Premature Reduction of the Pharyngeal Pumping Rate. Localization in all sections of the pharynx as well as pharyngeal tissue raises the probability of direct interactions between silica NPs and pharyngeal function, *i.e.*, pumping. Pharyngeal pumping serves food intake, and the respective pumping rate represents a sensitive measure to distinguish between conditions such as aging processes that are characterized by a linear rate reduction over time[32,33] or acute hunger responses that manifest in an immediate and significant rate reduction to a low pumping level.[34]

C. elegans were cultivated with H_2O, unlabeled silica NPs or BULK-silica for up to 7 days, and the pharyngeal pumping rate determined as pumps/minute each day (Figure 4). Every experiment additionally contained a cohort of animals that were left without food as hunger controls. Quantification of pharyngeal pumping shows a normal, age-correlated decline of the pumping rate from values above 200 pumps/min in 2 day-old untreated worms to below 150 pumps/min in 7-day old untreated worms (Figure 4A). This contrasts the hunger control that is not age-correlated and fluctuates at around 50 pumps/min from day 2 to day 7 (Figure 4A, black bars). A normal, age-related decline of pumping values is observed in H_2O, silica NP and BULK-silica-treated animals until day 3; however, between day 3 and day 4, pharyngeal pumping is significantly reduced in silica NP-exposed worms in comparison with the other cohorts and also declines faster (Figure 4A–E′). Thus, the lower pumping rate after silica NP treatment of 143 pumps/minute at day 4 is not reached until day 5, *i.e.*, 31 h later, in H_2O- and BULK-silica-treated *C. elegans* (Figure 4E). Comparison of the pumping events between the groups shows that 4-day old worms treated with silica NPs perform an average of 38 pumps/min less than their untreated or BULK-silica-treated counterparts (Figure 4E′). Reduced pharyngeal pumping of silica NP-treated *C. elegans* prevails from day 4 to 7. The results indicate that silica

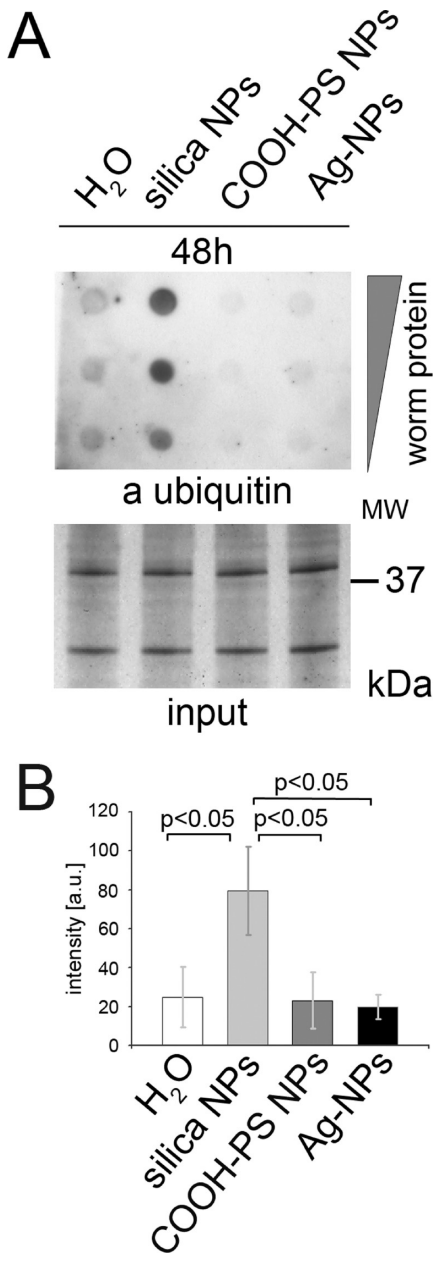

Figure 5. Silver and polystyrene NPs do not induce aggregation of SDS-insoluble ubiquitinated proteins in *C. elegans*. Filter retardation assays were detected with antibodies against ubiquitin. Accumulation of SDS-insoluble ubiquitinated proteins occurs in *C. elegans* treated with 2.5 mg/mL silica NPs for 48 h, in contrast to 2.5 mg/L Ag NPs or 2.5 mg/mL COOH-polystyrene NPs. Lower panel: as loading control, total protein extracts were separated by SDS-PAGE and detected by silver staining. (B) Respective densitometric quantification of filter retardation assays in (A). Values of three independent experiments are normalized to the H_2O-treated worms and represent means ± SD (24 h H_2O, COOH-polystyrene NPs and Ag NPs *versus* silica NPs, one way ANOVA with Tukey post-hoc test $p < 0.05$). Ag, silver; a.u., arbitrary units; COOH, carboxy; h, hours; kDA, kilodalton; MW, molecular weight; PS, polystyrene.

NPs interfere with pharyngeal function by premature initiation of an age-related reduction of pharyngeal pumping. This response clearly differs from starvation, due to the lack of similarity to the hunger curve (Figure 4). It is concluded that although silica NPs are abundant in the intestine, they do not induce starvation by perturbation of food intake. Rather silica NPs located in the pharynx have the potential to directly interfere with pharyngeal function by untimely, premature induction of the age-related decline of pumping.

To strengthen this conclusion, *C. elegans* were divided into different behavioral phenotypes that account for stochastic aging processes.[35] Adult worms were grouped into fast, low or not pumping, and pharyngeal pumping was monitored as described.[32] Untreated worms show declining numbers of fast-pumpers from day 2 to day 7, whereas the fraction of low-pumpers increased over time (Figure 4F). The curves cross between day 6 and day 7. The number of non-pumpers increases steadily, but on a lower level. In comparison, the silica NP-treated cohort loses the fast-pumpers earlier, and accumulates low-pumpers significantly (Figure 4G; Figure S6). As a result, both curves already cross between days 5 and 6 (Figure 4G). This is consistent with the idea that silica NPs induce the age-related decline of pharyngeal pumping prematurely.

The results support the notion that silica NP-treated worms prematurely develop aging-associated phenotypes. Notably, respective behavioral phenotypes are correlated with the local distribution of NPs: silica NPs accumulate in the pharynx inducing premature reduction of pharyngeal pumping, and localize in vulval cells where they increase frequency of the egg laying phenotype internal hatch, *i.e.*, 'bag of worms'.[19] Investigations are ongoing to identify the underlying mechanisms. Since adult worms are fully developed before their exposition with particles, NP-induced failure of respective organ function due to developmental defects can be excluded. Rather the results identify aging processes as targets of NP interactions. The molecular aging phenotype of altered protein homeostasis that occurs as early as 24 h after exposition with silica NPs is certainly one of several promising pathways to follow up on. Pharyngeal pumping and egg laying are behavioral end points of well-defined neuromuscular circuits[36,37] that might constitute targets of protein aggregation and neurodegeneration. Consistent with this idea, we showed previously that the silica NP-induced phenotype of internal hatch can be rescued by ethosuximide,[19] an anticonvulsive drug that significantly prolongs the lifespan of *C. elegans*.[38]

Screening of Different NPs for Their Ability To Induce Protein Aggregation in *C. elegans*. Screening of NPs with varying properties represents another valuable tool to identify the mechanisms of silica NP biointeraction in the worm. *C. elegans* were fed with 2.5 mg/mL unlabeled silica and carboxylated(COOH)-polystyrene or 2.5 mg/L silver(Ag) NPs for 48 h, collected, and biochemically analyzed by filter retardation assays (Figure 5A). While silica NP-treated *C. elegans* accumulate SDS-resistant, insoluble ubiquitinated proteins that are trapped on the cellulose acetate filters, neither COOH-polystyrene nor Ag NP-exposed worms show significant signals (Figure 5A,B). These results together with equal loading controls (Figure 5A, bottom, silver gel) suggest that nanomaterials differ concerning their ability to induce insoluble ubiquitinated proteins or protein aggregation. An as yet to be defined surface property of silica NPs facilitates intracellular interactions that are characterized by an increase of protein insolubility, and aggregation of endogenous proteins.

CONCLUSIONS

In the present study, premature aging phenotypes are identified as the consequence of exposing the nematode *C. elegans* to silica NPs. At the molecular level, protein homeostasis is altered by a shift of the equilibrium to more insoluble ubiquitinated proteins and formation of SDS-resistant protein aggregates. Presence of silica NPs in tissue and cells of the pharynx or the *vulva* is correlated with altered organ function such as premature reduction of pharyngeal pumping and egg laying behavior, respectively. While analyses of NP-related changes alone do not define the underlying mechanisms, these analyses are an essential element of investigations that have the potential to identify causal relationships and common pathways which can be tested across species. The model organism *C. elegans* has a proven record in this respect.[39,40] As demonstrated here, the transparency of the nematode allows for correlation between single-cell NP load and phenotypes from the molecular to the behavioral level. Thus, we introduce molecular and behavioral aging phenotypes in *C. elegans* as tools for both (i) further investigations of the NP biointerface and (ii) screening of engineered nanomaterials, *i.e.*, their properties.

MATERIALS AND METHODS

Particles. Silica NPs (50 nm diameter; unlabeled, rhodamine-labeled or FITC-labeled) and BULK-silica particles (500 nm diameter; unlabeled or rhodamine-labeled) were purchased from Kisker (Steinfurt, Germany), COOH-polystyrene(PS) NPs (50 nm diameter, unlabeled or yellow-orange-labeled) were from Polyscience (Warrington, PA, USA), and silver NPs (70 nm diameter, unlabeled) were purchased from Particular (Hannover, Germany). All particles were analyzed by dynamic light scattering in distilled H_2O using the Zetasizer Nano-ZS

(Malvern Instruments Ltd.) as detailed in Supporting Information (Table S1).

Animals. *C. elegans* wild-type N2 were kindly provided by the *Caenorhabditis* Genetic Center stock collection, University of Minnesota, St. Paul, MN, USA.

Worm Cultivation and Particle Treatment. *C. elegans* were cultured under standard conditions on NGM-agar plates supplemented with yeast extract and seeded with a lawn of *Escherichia coli* strain OP50 as food source. For all experiments, *C. elegans* were synchronized with hypchochlorite and cultured at 20 °C.[41,42] Particle treatment including selection of NP concentration was performed as described previously[19] with slight modifications. Young adults (day one) were transferred onto NGM-plates and fed on OP50 supplemented with particles, rhodamine B or distilled H_2O as indicated. For filter retardation assays and Congo red staining, aged worm populations were synchronized as described above and grown from L4-larval stage on NGM-agar plates supplemented with yeast-extract and 40 μM FUDR to maintain synchronization.[43] For pharyngeal pumping experiments, the aged worm populations were kept synchronized by picking the worms onto a new NGM-agar plate every day. Dead animals and worms with internally hatched larvae were censored.

Filter Retardation Assays. Worms were collected, washed with M9, and spun down. Pelleted worms were frozen in liquid nitrogen for a few minutes to break the cuticle. Worms were resuspended in 1 mL of SDS-lysis buffer (150 mM NaCl, 10 mM Tris-HCl pH 8, 2% SDS, protease inhibitor), boiled for 10 min, and subjected to further lysis in a swing rocket with a 7 mm steal bead for 10 min. The lysate was cleared by centrifugation at 5000*g* for 5 min, boiled for 2 min, and diluted with SDS-lysis buffer. The worm extracts were loaded on a dot blot and filtered through a cellulose acetate membrane with 0.2 μm pore size. The membrane was washed twice in SDS-washing buffer (150 mM NaCl, 10 mM Tris-HCl pH8, 0.1% SDS), blocked in PBS/0.25% Tween/5% nonfat milk overnight and incubated with the indicated antibodies diluted in PBS/0.25% Tween/5% nonfat milk. Bound antibodies (anti-ubiquitin (Sigma) at 1:50; anti-ubiquitin (FK1) at 1:500) were detected *via* horseradish peroxidase coupled secondary antibodies and the ECL-system on X-ray-films. Signals on X-ray-films were scanned and inverted with Photoshop (Adobe), and regions of interest were analyzed with Metamorph image analysis software package (MSD Analytic Technologies). Mean values and standard deviations were calculated and plotted with Microsoft Excel. Micrographs were assembled in Photoshop. Additional specificity controls of filter retardation assays were performed with aged, rhodamine-treated and/or starved adult *C. elegans* (Figure S7).

Purification of SDS-Insoluble Proteins. SDS-insoluble proteins were isolated *via* filter retardation assay followed by incubation of the membrane in 6 M guanidine HCl for 18 h at 18 °C. Eluted proteins were mixed with 2× loading buffer, boiled, separated by 4−20% SDS-gradient gels, and subjected to silver staining.

Microscopy. Living *C. elegans* were transferred to 5% agarose pads supplemented with 10 μM NaN_3 or embedded in agarose and analyzed at room temperature. For fixation procedures, worms were transferred onto poly-L-lysine coated objective slides, prefixed in 8% formaldehyde, subjected to freeze-cracking, and fixed by methanol/acetone. The worms were stained with 0.7 mg/mL Congo red/PBS to label amyloid proteins and/or 4′,6-diamidino-2-phenylindole (DAPI) that binds to A-T rich regions of the DNA helix, mounted with Vectashield (Vector Laboratories, Burlingame, CA, USA), and imaged. Imaging was performed using a confocal laser scanning microscope (Fluoview, IX70, Olympus) with a 60×/1.4NA Plan Apo objective or a LSM 510 confocal laser scanning microscope with a 40×/1.3NA Plan Neofluar objective (Zeiss). Light sheet microscopy was performed with the Lightsheet Z.1 from Zeiss. Congo red labeling was recorded with 568 nm excitation and magnifications of single intestinal nuclei are presented as inverted grayscale and pseudocolor intensity map using Metamorph and Photoshop. Single vulval cells were identified as described previously.[44]

Pharyngeal Pumping. For pharyngeal pumping experiment,s synchronized *C. elegans* were exposed to particles as described on day one of adulthood. As positive control (hunger), untreated worms were placed onto NGM-plates without OP50. The pharyngeal pumping rate was counted for 15 s by observation of single worms through a Zeiss stereomicroscope. One pump was defined as one contraction of the posterior bulb/grinder.[32,43] The measured values were extrapolated and projected to 1 min. Pharyngeal pumping was classified as previously described[32] with slight modifications: fast pharyngeal pumping (>36 pumps/15 s), slow (2−36 pumps/15 s) and none (<2 pumps/15 s). The mean values and the standard deviations were calculated and plotted with Microsoft Excel. The boxplots for day 3, 4, and 5 were assembled with Origin 8.5 (Origin Lab Corporation). In at least 3 independent experiments per treatment, a total of 43−160 animals were analyzed (H_2O, n = 160; silica NPs, n = 160, BULK-silica, n = 115; hunger, n = 43). Blind experiments were performed for all experiments, *i.e.*, without knowledge of worm treatment.

Statistical Analysis. Statistical significance was determined *via* Student's *t* test (Microsoft Excel) or one way ANOVA with Tukey post-hoc test (Origin 8.5, Origin Lab Corporation). *P*-values below 0.05 are considered as significant.

Conflict of Interest: The authors declare no competing financial interest.

Acknowledgment. We thank M. Kemnitz (Heinrich-Heine-University Duesseldorf) for help with dynamic light scattering analysis, S. Poppelreuther (Zeiss) for help with light sheet microscopy, and the Center for Advanced Imaging (CAI) at Heinrich-Heine-University Duesseldorf for kind support. Work in the von Mikecz laboratory is supported by the German Science Foundation (DFG) through grants (MI 486/7-1) and GRK 1033.

Supporting Information Available: Table S1 shows particle characterization by dynamic light scattering analysis. Figures S2−S7 address cellular and subcellular distribution of fluorescently labeled polystyrene NPs in living *C. elegans* (S2), time kinetics of silica NP distribution (S3), translocation of fluorescently labeled silica-NPs to the next generation *via* food intake (S4), distribution of BULK silica (S5), silica NP-induced accumulation of low pumpers (S6), and specificity controls of filter retardation assays (hunger, rhodamine B; S7). This material is available free of charge *via* the Internet at http://pubs.acs.org.

REFERENCES AND NOTES

1. Baun, A.; Hartmann, N. B.; Grieger, K.; Kusk, K. O. Ecotoxicity of Engineered Nanoparticles to Aquatic Invertebrates: A Brief Review and Recommendations for Future Toxicity Testing. *Ecotoxicology* **2008**, *17*, 387–395.
2. Leeuw, T. K.; Reith, R. M.; Simonette, R. A.; Harden, M. E.; Cherukuri, P.; Tsyboulski, D. A.; Beckingham, K. M.; Weisman, R. B. Single-Walled Carbon Nanotubes in the Intact Organism: Near-IR Imaging and Biocompatibility Studies in *Drosophila*. *Nano Lett.* **2007**, *7*, 2650–2654.
3. Huang, H.; Delikanli, S.; Zeng, H.; Ferkey, D. M.; Pralle, A. Remote Control of Ion Channels and Neurons through Magnetic-Field Heating of Nanoparticles. *Nat. Nanotechnol.* **2010**, *5*, 602–606.
4. Schleh, C.; Semmler-Behnke, M.; Lipka, J.; Wenk, A.; Hirn, S.; Schäffler, M.; Schmid, G.; Simon, U.; Kreyling, W. G. Size and Surface Charge of Gold Nanoparticles Determine Absorption Across Intestinal Barriers and Accumulation in Secondary Target Organs After Oral Administration. *Nanotoxicology* **2012**, *6*, 36–46.
5. van Aerle, R.; Lange, A.; Moorhouse, A.; Paszkiewicz, K.; Ball, K.; Johnston, B. D.; de-Bastos, E.; Booth, T.; Tyler, C. R.; Santos, E. M. Molecular Mechanisms of Toxicity of Silver Nanoparticles in Zebrafish Embryos. *Environ. Sci. Technol.* **2013**, *47*, 8005–8014.
6. Lim, S. F.; Riehn, R.; Ryu, W. S.; Khanarian, N.; Tung, C. K.; Tank, D.; Austin, R. H. *In Vivo* and Scanning Electron Microscopy Imaging of Upconverting Nanophosphors in *Caenorhabditis elegans*. *Nano Lett.* **2006**, *6*, 169–174.
7. Mohan, N.; Chen, C. S.; Hsieh, H. H.; Wu, Y. C.; Chang, H. C. *In Vivo* Imaging and Toxicity Assessments of Fluorescent

Nanodiamonds in *Caenorhabditis elegans*. *Nano Lett.* **2010**, *10*, 3692–3699.
8. Donner, J. S.; Thompson, S. A.; Alonso-Ortega, C.; Morales, J.; Rico, L. G.; Santos, S. I.; Quidant, R. Imaging of Plasmonic Heating in a Living Organism. *ACS Nano* **2013**, *7*, 8666–8672.
9. Kim, S. W.; Kwak, J. I.; An, Y. J. Multigenerational Study of Gold Nanoparticles in *Caenorhabditis elegans*: Transgenerational Effect of Maternal Exposure. *Environ. Sci. Technol.* **2013**, *47*, 5393–5399.
10. Zanni, E.; De Bellis, G.; Bracciale, M. P.; Broggi, A.; Santarelli, M. L.; Sarto, M. S.; Palleschi, C.; Uccelletti, D. Graphite Nanoplatelets and *Caenorhabditis elegans*: Insights from an *in Vivo* Model. *Nano Lett.* **2012**, *12*, 2740–2744.
11. The *C. elegans* Sequencing Consortium. Genome Sequence of the Nematode *C. elegans*: A Platform for Investigating Biology. *Science* **1998**, *282*, 2012-2018.
12. Sulston, J. E.; Horvitz, H. R. Post-Embryonic Cell Lineages of the Nematode *Caenorhabditis elegans*. *Dev. Biol.* **1977**, *56*, 110–156.
13. Schafer, W. R. Deciphering the Neural and Molecular Mechanisms of *C. elegans* Behavior. *Curr. Biol.* **2005**, *15*, R723–729.
14. Shu, X.; Lev-Ram, V.; Deerinck, T. J.; Qi, Y.; Ramko, E. B.; Davidson, M. W.; Jin, Y.; Ellisman, M. H.; Tsien, R. Y. A Genetically Encoded Tag for Correlated Light and Electron Microscopy of Intact Cells, Tissues and Organisms. *PLoS Biol.* **2011**, *9*, e1001041.
15. Kenyon, C. The First Long-Lived Mutants: Discovery of the Insulin/IGF-1 Pathway for Ageing. *Philos. Trans. R. Soc. London, Ser. B* **2011**, *366*, 9–16.
16. Lund, J.; Tedesco, P.; Duke, K.; Wang, J.; Kim, S. K.; Johnson, T. E. Transcriptional Profile of Aging in *C. elegans*. *Curr. Biol.* **2002**, *12*, 1566–1573.
17. Reis-Rodrigues, P.; Czerwieniec, G.; Peters, T. W.; Evani, U. S.; Alavez, S.; Gaman, E. A.; Vantipalli, M.; Mooney, S. D.; Gibson, B. W.; Lithgow, G. J.; *et al.* Proteomic Analysis of Age-Dependent Changes in Protein Solubility Identifies Genes That Modulate Lifespan. *Aging Cell* **2012**, *11*, 120–127.
18. David, D. C.; Ollikainen, N.; Trinidad, J. C.; Cary, M. P.; Burlingame, A. L.; Kenyon, C. Widespread Protein Aggregation as an Inherent Part of Aging in *C. elegans*. *PLoS Biol.* **2010**, *8*, e1000450.
19. Pluskota, A.; Horzowski, E.; Bossinger, O.; von Mikecz, A. *Caenorhabditis elegans* Nanoparticle-Bio-Interactions Become Transparent: Silica-Nanoparticles Induce Reproductive Senescence. *PLoS One* **2009**, *4*, e6622.
20. Roh, J. Y.; Sim, S. J.; Yi, J.; Park, K.; Chung, K. H.; Ryu, D. Y.; Choi, J. Ecotoxicity of Silver Nanoparticles on the Soil Nematode *Caenorhabditis elegans* Using Functional Ecotoxicogenomics. *J. Environ. Sci. Technol.* **2009**, *43*, 3933–3940.
21. Wang, H.; Wick, R. L.; Xing, B. Toxicity of Nanoparticulate and Bulk ZnO, Al_2O_3 and TiO_2 to the Nematode *Caenorhabditis elegans*. *Environ. Pollut.* **2009**, *157*, 1171–1177.
22. Qu, Y.; Li, W.; Zhou, Y.; Liu, X.; Zhang, L.; Wang, L.; Li, Y. F.; Iida, A.; Tang, Z.; Zhao, Y.; *et al.* Full Assessment of Fate and Physiological Behavior of Quantum Dots Utilizing *Caenorhabditis elegans* as a Model Organism. *Nano Lett.* **2011**, *11*, 3174–3183.
23. Hemmerich, H.; von Mikecz, A. Defining the Subcellular Interface of Nanoparticles by Live-Cell Imaging. *PLoS One* **2013**, *8*, e62018.
24. Wanker, E. E.; Scherzinger, E.; Heiser, V.; Sittler, A.; Eickhoff, H.; Lehrach, H. Membrane Filter Assay for Detection of Amyloid-like Polyglutamine-Containing Protein Aggregates. *Methods Enzymol.* **1999**, *309*, 375–386.
25. Linse, S.; Cabaleiro-Lago, C.; Xue, W. F.; Lynch, I.; Lindman, S.; Thulin, E.; Radford, S. E.; Dawson, K. A. Nucleation of Protein Fibrillation by Nanoparticles. *Proc. Natl. Acad. Sci. U.S.A.* **2007**, *104*, 8691–8696.
26. Chen, M.; von Mikecz, A. Formation of Nucleoplasmic Protein Aggregates Impairs Nuclear Function in Response to SiO_2 Nanoparticles. *Exp. Cell Res.* **2005**, *305*, 51–62.
27. Chen, M.; Singer, L.; Scharf, A.; von Mikecz, A. Nuclear Polyglutamine-Containing Protein Aggregates as Active Proteolytic Centers. *J. Cell Biol.* **2008**, *180*, 697–704.
28. Nel, A. E.; Mädler, L.; Velegol, D.; Xia, T.; Hoek, E. M.; Somasundaran, P.; Klaessig, F.; Castranova, V.; Thompson, M. Understanding Biophysicochemical Interactions at the Nano-Bio Interface. *Nat. Mater.* **2009**, *8*, 543–557.
29. Nabeshi, H.; Yoshikawa, T.; Matsuyama, K.; Nakazato, Y.; Matsuo, K.; Arimori, A.; Isobe, M.; Tochigi, S.; Kondoh, S.; Hirai, T.; *et al.* Systemic Distribution, Nuclear Entry and Cytotoxicity of Amorphous Nanosilica Following Topical Application. *Biomaterials* **2011**, *32*, 2713–2724.
30. Contreras, E. Q.; Cho, M.; Zhu, H.; Puppala, H. L.; Escalera, G.; Zhong, W.; Colvin, V. L. Toxicity of Quantum Dots and Cadmium Salt to *Caenorhabditis elegans* after Multigenerational Exposure. *Environ. Sci. Technol.* **2013**, *47*, 1148–1154.
31. Minullina, R. T.; Osin, Y. N.; Ishmuchametova, D. G.; Fakhrullin, R. F. Interfacing Multicellular Organisms with Polyelectrolyte Shells and Nanoparticles: A *Caenorhabtidis elegans* Study. *Langmuir* **2011**, *27*, 7708–7713.
32. Huang, C.; Xiong, C.; Kornfeld, K. Measurements of Age-Related Changes of Physiological Processes That Predict Lifespan of *Caenorhabditis elegans*. *Proc. Natl. Acad. Sci. U. S.A.* **2004**, *101*, 8084–8089.
33. Collins, J. J.; Huang, C.; Hughes, S.; Kornfeld K. Measurement and Analysis of Age-Related Changes in *Caenorhabditis elegans*. In *WormBook* [Online]; The C. elegans Research Community, WormBook, 2008; pp 1−21. DOI: 10.1895/wormbook.1.137.1.
34. Donohoe, D. R.; Jarvis, R. A.; Weeks, K.; Aamodt, E. J.; Dwyer, D. S. Behavioral Adaptation in *C. elegans* Produced by Antipsychotic Drugs Requires Serotonin and Is Associated with Calcium Signalling and Calcineurin Inhibition. *Neurosci. Res.* **2009**, *64*, 280–289.
35. Herndon, L. A.; Schmeissner, P. J.; Dudaronek, J. M.; Brown, P. A.; Listner, K. M.; Sakano, Y.; Paupard, M. C.; Hall, D. H.; Driscoll, M. Stochastic and Genetic Factors Influence Tissue-Specific Decline in Ageing *C. elegans*. *Nature* **2002**, *419*, 808–814.
36. Niacaris, T.; Avery, L. Serotonin Regulates Repolarization of the *C. elegans* Pharyngeal Muscle. *J. Exp. Biol.* **2003**, *206*, 223–231.
37. Hobson, R. J.; Hapiak, V. M.; Xiao, H.; Buehrer, K. L.; Komuniecki, P. R.; Komuniecki, R. W. SER-7, a *Caenorhabditis elegans* 5-HT7-Like Receptor Is Essential for the 5-HT Stimulation of Pharyngeal Pumping and Egg Laying. *Genetics* **2006**, *172*, 159–169.
38. Evason, K.; Huang, C.; Yamben, I.; Covey, D. F.; Kornfeld, K. Anticonvulsant Medications Extend Worm Life-Span. *Science* **2005**, *307*, 258–262.
39. Kaletta, T.; Hengartner, M. O. Finding Function in Novel Targets: *C. elegans* as a Model Organism. *Nat. Rev. Drug Discovery* **2006**, *5*, 387–398.
40. Benedetto, A.; Au, C.; Avila, D. S.; Milatovic, D.; Aschner, M. Extracellular Dopamine Potentiates Mn-Induced Oxidative Stress, Lifespan Reduction, and Dopaminergic Neurodegeneration in a BLI-3-Dependent Manner in *Caenorhabditis elegans*. *PLoS Genet.* **2010**, *6*, e1001084.
41. Brenner, S. The Genetics of *Caenorhabditis elegans*. *Genetics* **1974**, *77*, 71–94.
42. Stiernagle, T. Maintenance of *C. elegans*. In *C. elegans*; Hope, I. A., Ed.; Oxford Biology Press: Oxford, New York, 1999; pp 51−67.
43. Honda, Y.; Tanaka, M.; Honda, S. Trehalose Extends Longevity in the Nematode *Caenorhabditis elegans*. *Aging Cell* **2010**, *9*, 558–569.
44. Inoue, T.; Sherwood, D. R.; Aspöck, G.; Butler, J. A.; Gupta, B. P.; Kirouac, M.; Wang, M.; Lee, P. Y.; Kramer, J. M.; Hope, I.; *et al.* Gene Expression Markers for *Caenorhabditis elegans* Vulval Cells. *Mech. Dev.* **2002**, *119* (Suppl 1), S203–209.